

A Synchronization-Desynchronization Code for Natural Communication Signals

Jan Benda,^{1,3,*} André Longtin,^{1,2} and Leonard Maler¹

¹Department of Cellular and Molecular Medicine

University of Ottawa

51 Smyth Road

Ottawa, Ontario K1H 8M5

Canada

²Department of Physics

University of Ottawa

150 Louis Pasteur

Ottawa, Ontario K1N 6N5

Canada

³Institute for Theoretical Biology

Humboldt University

Invalidenstrasse 43

10115 Berlin

Germany

Summary

Synchronous spiking of neural populations is hypothesized to play important computational roles in forming neural assemblies and solving the binding problem. Although the opposite phenomenon of desynchronization is well known from EEG studies, it is largely neglected on the neuronal level. We here provide an example of *in vivo* recordings from weakly electric fish demonstrating that, depending on the social context, different types of natural communication signals elicit transient desynchronization as well as synchronization of the electroreceptor population without changing the mean firing rate. We conclude that, in general, both positive and negative changes in the degree of synchrony can be the relevant signals for neural information processing.

Introduction

Important features of spiking neurons are their ability to synchronize (e.g., Ermentrout, 1996; Volgushev et al., 1998; Tamás et al., 2000; Lindner et al., 2005; Galán et al., 2006), their ability to detect synchronous input (Bernander et al., 1994; Perez-Orive et al., 2004; Galarreta and Hestrin, 2001; Azouz and Gray, 2003), and their ability to transmit synchronous spikes (Aertsen et al., 1996). Synchronous spiking can be caused by common, often periodic, stimulation of a population of (independent) neurons or generated internally by network dynamics.

Stimulus-induced synchronous discharge may contribute to coding. For example, in retinal ganglion cells, considerably more information can be extracted about a stimulus if synchronous spikes are considered separately (Dan et al., 1998), and fixation movement-induced synchrony improves feature estimation (Greschner et al., 2002). The utility of synchronous discharge has recently been demonstrated in that the escape behavior

of frogs was shown to rely on synchrony of a specific class of ganglion cells (Ishikane et al., 2005).

Internally generated synchrony, possibly at particular phases relative to a global oscillatory output, is hypothesized to bind neurons into dynamical cell assemblies (see Harris, 2005 for a review). This idea has been thoroughly investigated in the visual system (Singer and Gray, 1995; Singer, 1999) in the context of the “binding problem” of different stimulus features (Robertson, 2003) and is supported by many experimental studies, from the representation of moving bars in area 17 of cats (Engel et al., 1992) to higher-level integration of faces in inferior temporal cortex (Hirabayashi and Miyashita, 2005). Some studies, however, failed to confirm the “binding by synchrony” hypothesis (Lamme and Spekreijse, 1998; Thiele and Stoner, 2003).

In the olfactory system, odorants have been reported to induce oscillatory activity with transient, dynamic synchronization of odor-specific neural assemblies (Laurent, 1996). Synchronous and asynchronous spikes appeared to be carrying qualitatively different information about the odorant (Friedrich et al., 2004).

Although synchronized discharge has received much focus, to our knowledge, there is only a single report suggesting that desynchronization might also be important for specific kinds of neural processing (Ackert et al., 2006). However, in this paper, *in vivo* recordings in weakly electric fish demonstrate concrete sensory coding mechanisms that utilize either synchronization or desynchronization, respectively, of neuronal discharge in response to two distinct and behaviorally important classes of natural communication signals.

Weakly electric fish generate an electric organ discharge (EOD) that they use for electrolocation (Nelson and MacIver, 1999) as well as for communication. In wave-type electric fish, the EOD is a continuous periodic signal with constant amplitude whose frequency is species- and sex-specific. In our model system, the gymnotiform species *Apteronotus leptorhynchus*, males discharge at higher frequencies (800 to 1000 Hz) than females (500 to 750 Hz) (Meyer et al., 1987). The superposition of the EODs of two fish results in a beat, a periodic amplitude modulation with frequency Δf given by the difference of the frequencies of the two individual EODs. Thus, beat frequencies experienced during the interaction with the same sex are typically smaller (less than 50 Hz) than beat frequencies during interaction with the opposite sex (more than 50 Hz). Behavioral studies have shown that these fish and related species are able to discriminate between the EOD frequencies of conspecifics (Heiligenberg and Partridge, 1981; Kramer, 1999). These fish can therefore use the beat frequency in order to infer the sex of a conspecific.

In addition to the beat, *A. leptorhynchus* can actively modulate its EOD frequency for communication purposes (Zakon et al., 2002; Zupanc, 2002; Oestreich et al., 2006). During one class of EOD modulation, chirps, the EOD frequency is transiently increased. Two main categories of brief (about 20 ms) chirps are known from behavioral studies: “small chirps,” where the EOD

*Correspondence: j.benda@biologie.hu-berlin.de

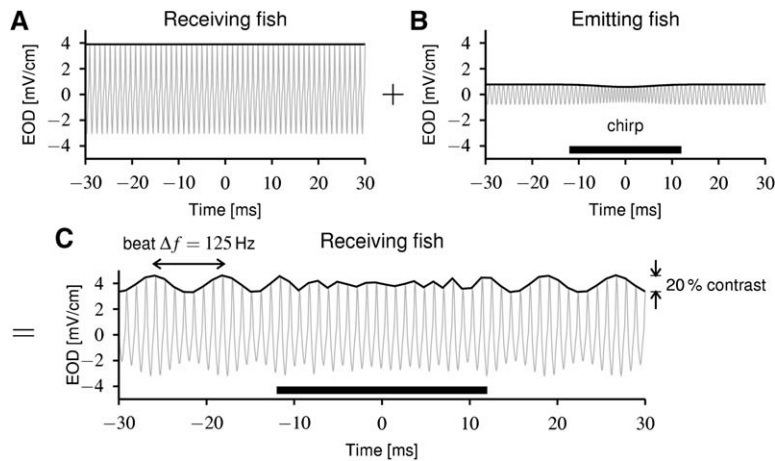


Figure 1. The Stimulus

(A) An individual fish experiences its own EOD (gray line) with constant amplitude (black line).

(B) The EOD of a distant fish has a smaller amplitude (here 20%) at the location of the receiving fish. This distant fish emits a large chirp (thick horizontal bar) that reduces the amplitude by 25% and increases the frequency by 600 Hz during 24 ms. Shown is an artificially designed chirp signal that we used as a stimulus for the electrophysiological recordings.

(C) The superposition of the two wave forms of the receiving fish (A) and the emitting fish (B) is the effective electric field that stimulates the electroreceptors of the receiving fish. A beat is created (here with frequency $\Delta f = 125$ Hz) that is disrupted during the large chirp (thick horizontal bar); this amplitude modulation (black line) is what we refer to as the “stimulus” in this paper and is shown in the remaining figures as “EOD AM.” Note that the AM fades away during the large chirp.

frequency is increased by about 100 Hz, and “large chirps,” where the EOD frequency is increased by as much as 600 Hz (Hagedorn and Heiligenberg, 1985; Zupanc and Maler, 1993; Engler et al., 2000; Bastian et al., 2001; Zupanc, 2002; Triefenbach and Zakon, 2003). These frequency modulations lead to strong amplitude modulations (AMs) when superimposed with another EOD. Small chirps are emitted mainly at beat frequencies below 50 Hz and are hypothesized to be aggressive signals. Large chirps, on the other hand, are also emitted by males but in response to the higher beat frequencies (>50 Hz; Bastian et al., 2001; Triefenbach and Zakon, 2003) that are typical for male-female interactions. Thus, in addition to the beat frequency, these fish can also use transient EOD modulations as signals related to aggression and perhaps courtship (Hagedorn and Heiligenberg, 1985; Bastian et al., 2001). Note that similar modulations of a carrier are observed in natural acoustic stimuli (e.g., Bar-Yosef et al., 2002).

AMs of the EOD as induced by beats and chirps are detected by tuberous electroreceptors that are tuned to the individual fish’s EOD frequency (Hopkins, 1976). Most of these receptors code for EOD AMs by varying the probability of their discharge (P-units) (Hagiwara et al., 1965; Scheich et al., 1973; Bastian, 1981; Nelson et al., 1997).

We here investigate how beats of various frequencies are represented by the population of P-unit afferents and thus discriminate between males and females, and how two classes of very brief modulations as caused by either small or large chirps are coded by the P-unit population. Our results emphasize that the degree of synchrony as well as changes in synchrony, in particular a transient desynchronization, might most likely be the relevant code for natural communication signals such as chirps.

Results

Desynchronization by Large Chirps

The EOD amplitude of isolated fish is constant (Figure 1A). The superposition of the EODs of males and females results in amplitude modulations (beats) with

frequencies that are usually higher than about 50 Hz. In this situation the male will emit large chirps (Figure 1B). Such a chirp lasts for about 20 ms, during which the frequency of the EOD is increased by about 600 Hz and the amplitude of the EOD is decreased by about 25% (Bastian et al., 2001; Triefenbach and Zakon, 2003). The reduction of the male’s EOD amplitude during the chirp will result in a reduction of the EOD AM received by the female. In addition, the increase in the male’s EOD frequency transiently increases the frequency difference to $\Delta f \approx 700$ Hz, and thus, the beat frequency is close to the female’s own EOD frequency (typically <800 Hz). One way of understanding the shape of the resulting waveform on the female’s body (Figure 1C) is that this high-frequency beat cannot be properly sampled by the female’s own EOD frequency (i.e., the female’s EOD frequency is below the critical Nyquist sampling frequency for the beat: 2×700 Hz).

In summary, females can identify males by the fast beat (>50 Hz) produced by the superimposition of their EODs. Male large chirps will interrupt this fast beat by reducing the amplitude of the beat and changing its temporal structure for less than 25 ms. In what follows, we describe how these signals are encoded by the P-unit electroreceptors.

Spike raster plots obtained from single-unit recordings (Figure 2) demonstrate that P-unit spikes lock to the beat and thus become synchronized to the beat pattern. A large chirp reduces the stimulus amplitude and desynchronizes the spike response. During the chirp, the spiking activity is similar to the apparently random baseline activity (left column) that is well known from the probabilistic nature of P-unit firing (Scheich et al., 1973; Nelson et al., 1997).

The time course of the firing rate (Figure 2C) was computed by convolving the spike trains with a Gaussian kernel and averaging over trials. A narrow kernel with a standard deviation of 1 ms approximately matches the fast component of P-unit-evoked excitatory postsynaptic potentials (EPSPs) in target cells, whereas a wider kernel with a standard deviation of 5 ms matches the second fastest (excitatory or inhibitory) potential

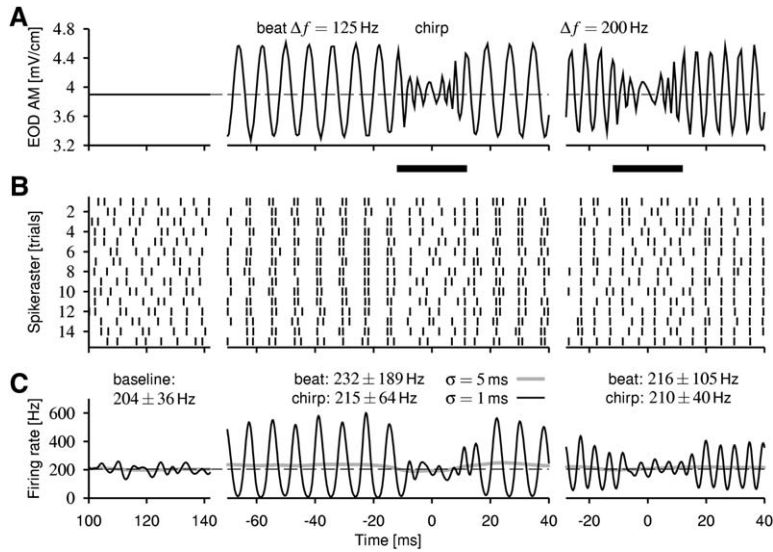


Figure 2. Large Chirps Desynchronize Single-Unit Electroreceptor Response

(A) The EOD amplitude modulation of an isolated fish is constant (left column). A large chirp emitted by a second fish (centered around time $t = 0$, thick horizontal bar) interrupts the beat that arises from the superposition of the EODs of the two communicating fish. Beat contrast is 20% and beat frequency is $\Delta f = 125$ Hz in the middle column (same as in Figure 1C) and $\Delta f = 200$ Hz in the right column. (B) Spike raster recorded from a single electroreceptor. The response of this unit shows approximately 2:1 locking to the 125 Hz beat (middle column) and 1:1 locking to the 200 Hz beat (right column) that is interrupted by a brief period of asynchrony during the chirp. (C) Firing rate computed by convolving the spike trains from the single-unit recording (B) with Gaussian kernels with standard deviations of 1 ms (black line) and 5 ms (gray line) and averaging over trials. The dashed line is the mean firing rate computed from 8.5 s of baseline activity. The labels above the panel indicate the temporal mean and standard deviation (modulation depth) of the firing rate (1 ms kernel) computed during baseline activity, beat, and chirp.

(Berman and Maler, 1998). The firing rate computed with the 1 ms kernel (black line) is strongly modulated during the beat, and its periodic time course exactly matches that of the beat. The modulation depth of the firing rate and the degree of P-unit synchrony depends on the beat frequency (compare middle and right column in Figure 2). The firing rate modulation is strongly reduced during the large chirp and becomes similar to baseline firing rate. In contrast, the firing rate computed using 5 ms kernels (gray line) as well as the mean firing rate hardly changes from baseline values during either the beat or large chirp.

Since all P-units became phase-locked to the beat in a similar manner, these results suggest that the activity of the whole P-unit population itself will also synchronize during a beat and that this synchronization will be lost during a large chirp. We therefore performed dual-unit

recordings and recordings of the population response in order to validate this “synchronization-desynchronization” hypothesis. Simultaneously recorded pairs of spike trains also become phase-locked and mutually synchronized during the high-frequency beat, and this synchronization is lost during the large chirp, where again, the firing pattern resembles the baseline discharge (Figure 3).

We quantified the degree of P-unit synchrony during baseline discharge, beats, and large chirps by computing the correlation coefficient (Equation 1) between pairs of spike train firing rates (1 ms Gaussian kernels). The duration of the P-unit-evoked EPSPs does not appear to change appreciably over the range of membrane potentials expected from synaptic input (Berman and Maler, 1998); thus, as expected, qualitatively similar results were obtained with 0.5 ms and 2 ms kernels. The

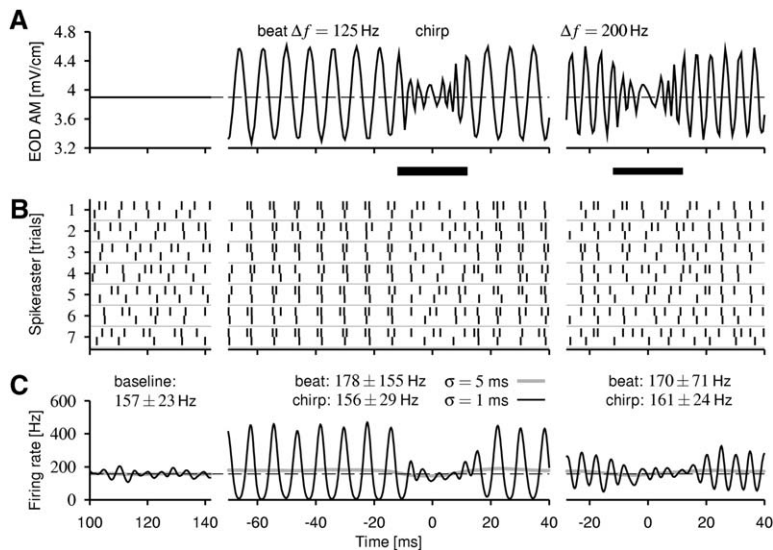


Figure 3. Large Chirps Desynchronize Dual-Unit Electroreceptor Response

(A) The stimuli. Left column: baseline EOD, middle column: $\Delta f = 125$ Hz, right column: $\Delta f = 200$ Hz at 20% contrast; same as in Figure 2.

(B) Spike raster of the two simultaneously recorded electroreceptors (0.22 and 0.12 spikes per EOD cycle during baseline activity). Each row (separated by horizontal gray lines) shows the simultaneously recorded spike trains of the two units. The upper spike trains are the same as shown in Figure 2B.

(C) The firing rate computed by averaging over the spike trains from both cells convolved with Gaussian kernels with a standard deviation of either 1 ms (black line) or 5 ms (gray line) reveals the desynchronization of the receptors’ response by the chirps.

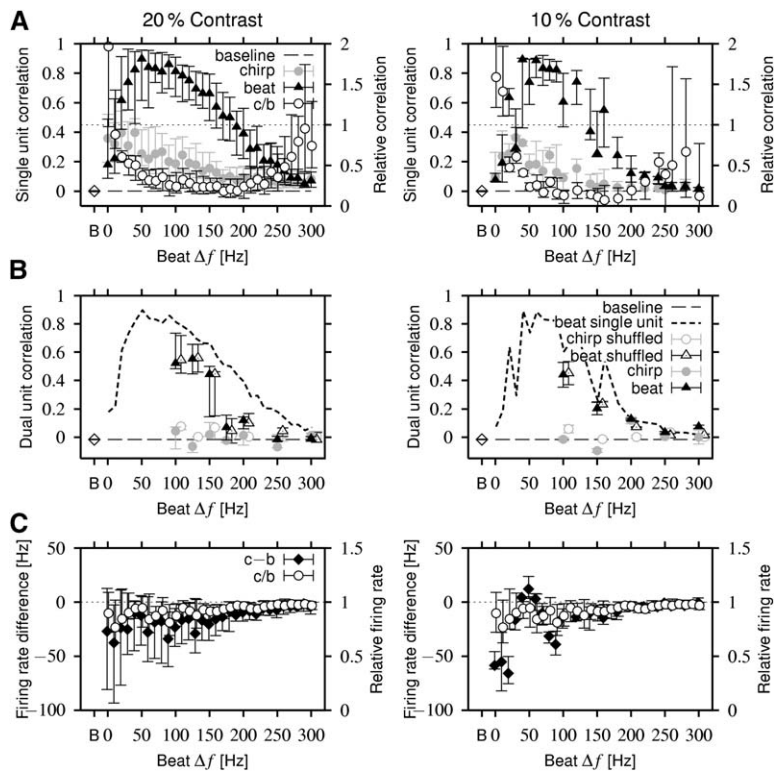


Figure 4. Summary of Single- and Dual-Unit Recordings for Large-Chirp Stimuli

Plotted are median values with the error bars marking the 1. and 3. quartile. The data points were measured at $\Delta f = 5, 10, 20, 30, \dots, 290, 300$ Hz beat frequency with 20% contrast (left column) and 10% contrast (right column). (A) Correlation on a 1 ms timescale of single-unit spike trains during chirps (gray circles) and beats (black triangles) obtained from multiple presentations of the same stimulus in comparison with baseline activity (diamond and dashed line). The open circles denote the median of the correlation during the chirp divided by the one during the beat (right axis); the fine dashed line marks a ratio of one. (B) Correlation computed from simultaneously recorded pairs of spike trains (filled symbols). Data points of nonsimultaneously (shuffled) recorded pairs are slightly shifted to the right (open symbols). (C) The difference of the mean firing rate during chirps minus the one during the beats (black diamonds) and the corresponding relative firing rate ratio (open circles, chirp divided by beat).

correlation coefficient equals one for perfect synchrony and is zero for correlations at chance level as given by the single-trial mean firing rates. For the single-unit recordings, we averaged over the correlation coefficients (estimated separately during beat and chirp) from all possible pairs of spike trains obtained from a single cell in response to multiple presentations of a single stimulus. Baseline P-unit activity of single-unit recordings is uncorrelated ($\bar{r} = 0.002 \pm 0.007$, $n = 79$ cells, not significantly different from zero, two-tailed sign test, $n_+ = 36$, $p > 0.4$). The beat, however, induces strong correlations; the 15 spike trains shown in the middle panel of Figure 2B have an averaged correlation coefficient of 0.80 (105 pairs) during the beat ($-80 \text{ ms} < t < -24 \text{ ms}$). This correlation is reduced to 0.18 during the chirp ($-5 \text{ ms} < t < 15 \text{ ms}$).

In the case of dual-unit recordings, we averaged over all pairs of simultaneously recorded spike trains. For the dual-unit recording shown in the left panel of Figure 3B, we get a correlation coefficient of -0.02 during baseline activity. For all P-unit pairs, baseline activity is uncorrelated ($\bar{r} = -0.01 \pm 0.01$, $n = 5$, not significantly different from zero, two-tailed sign test, $n_+ = 1$, $p > 0.3$), as would be expected given the short timescale of serial correlation (Ratnam and Nelson, 2000; Chacron et al., 2001) and adaptation (Nelson et al., 1997; Benda et al., 2005) of these afferents as previously reported (Chacron et al., 2005a). P-unit correlation rises to values of 0.63 ± 0.14 during beats with a frequency of 100 Hz at 20% contrast. During large chirps the correlation is again significantly reduced to -0.01 ± 0.10 (one-tailed Wilcoxon test, $p < 0.01$, $n = 7$), back to baseline level (two-tailed Wilcoxon test, $p > 0.9$, $n = 7$). This supports the hypothesis that the uncorrelated baseline P-unit discharge becomes synchronized (correlated) during

a high-frequency beat resulting from the proximity of the fish and desynchronized (uncorrelated) during a large chirp produced as a communication signal.

In order to quantify spike train correlation as a function of beat frequency, we recorded and analyzed single-unit responses to large-chirp stimuli at various beat frequencies chosen from a range of 5–300 Hz and two contrasts (10%, 20%) in 76 cells (23 ± 5 trials per stimulus, 18 ± 13 stimuli per cell, total number of stimuli $n = 1339$), resulting in 13 to 79 (average 38) stimuli per beat frequency at 20% contrast and from 3 to 16 (average 7) stimuli at 10% contrast. The correlation coefficients and firing rates computed from these data as a function of beat frequency are summarized in Figure 4.

The single P-unit correlation during the beat rises steeply from 5 to 50 Hz to values up to 0.9 (median) and, for beat frequencies >100 Hz, declines back to baseline levels (unstimulated) by ~ 250 Hz (Figure 4A). The correlations are significantly greater than baseline for all measured beat frequencies (one-tailed Wilcoxon test, $p \ll 0.001$ at 20% contrast, $p < 0.05$ at 10% contrast). In contrast, spike correlation during large chirps is in general low (median < 0.4) for all beat frequencies, but it is still significantly different from baseline correlation (two-tailed Wilcoxon test, $p \ll 0.001$ at 20% contrast, $p < 0.05$ at 10% contrast).

There is therefore a large region of beat frequencies ranging from 20 Hz to 260 Hz for 20% contrast (one-tailed Wilcoxon test, $p \ll 0.001$) and 40 to 240 Hz at 10% contrast (one-tailed Wilcoxon test, $p < 0.01$) in which the correlation during the beat is significantly higher than during the large chirp as expected from the raster plots (Figure 2B). Large chirps occurring during these beats strongly reduce the correlation by as much as 5-fold. This effect is almost independent of

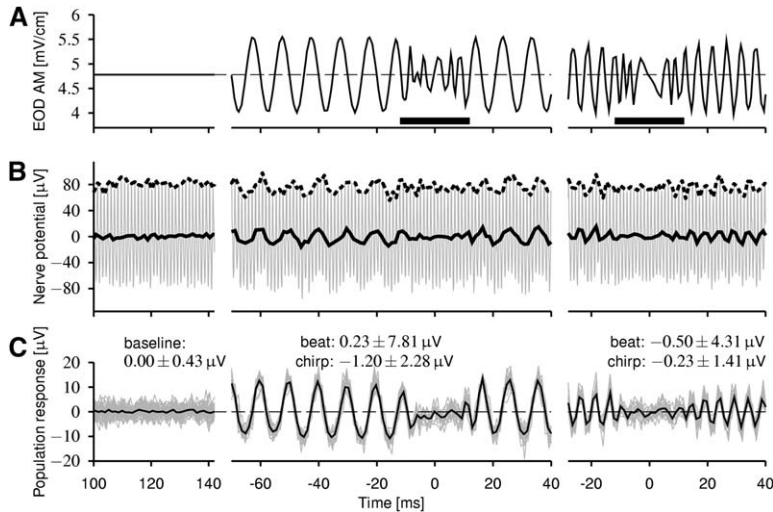


Figure 5. Large Chirps Desynchronize Population Response

(A) The stimuli. Left column: baseline EOD, middle column: $\Delta f = 100$ Hz, right column: $\Delta f = 200$ Hz at 20% contrast with large chirps at time $t = 0$ (thick horizontal bar).

(B) The plain hook electrode recording from the trunk electroreceptor nerve is contaminated with the EOD generated by the fish (solid gray line) that adds to the population response. Extracting the envelope (dashed line) from the peaks results in noisy signals, whereas a sliding average that is exactly one EOD cycle wide and thus removes the EOD component results in a clearer response (solid line).

(C) The population response (black line) is obtained from the nerve potentials filtered with the sliding average (gray lines, solid black line in [B]) by averaging over trials. The numbers indicate the temporal mean \pm standard deviation of the population response during baseline, beat, and chirp. The thin dashed line is the mean response measured during baseline EOD.

the two contrasts we tested (left column: 20%; right column: 10%). Thus, for the entire range of beat frequencies that is typical for male-female interaction, the uncorrelated baseline P-unit spike train becomes synchronized to the beats, and this synchrony is transiently reduced during the large chirps.

The same pattern is confirmed by dual-unit recordings from five pairs of cells (altogether $n = 31$ presented stimuli with 17 ± 4 trials per stimulus; 2 to 6 (average 4.4) stimuli per beat frequency were presented at 20% contrast and 2 stimuli at 10% contrast; results are summarized in Figure 4B, filled symbols). There is a high correlation between the cells during a beat with $\Delta f = 100$ Hz (median 0.52 at 20% contrast), whereas this correlation is completely eliminated during the chirps (median 0.04, significant difference: one-tailed Wilcoxon test, $p = 0.008$, $n = 7$). The correlation during the beat is significantly larger than during both the chirp and baseline activity up to beat frequencies of 200 Hz (one-tailed Wilcoxon test, $p < 0.05$, $n = 6$). This correlation is reduced to baseline levels by the large chirps (two-tailed Wilcoxon test, $p > 0.1$, $n = 5-7$). The correlations during the beat and the chirp obtained from the dual-unit recordings, however, are lower compared with those of the single-unit recordings (dashed line). This is not surprising, since the baseline rates of the electroreceptors are distributed over a range from 90 Hz to 460 Hz (79 cells), and thus, two simultaneously recorded units usually have quite different baseline rates (difference of 6–116 Hz for the five pairs).

The correlation coefficients (Equation 1) computed from shuffled, i.e., nonsimultaneously recorded spike trains from the dual-unit recordings (Figure 4B, open symbols), are indistinguishable from the ones computed from simultaneously recorded spike trains (two-tailed Wilcoxon test, $p > 0.3$, $n = 5-7$ for all measured beat frequencies at 20% contrast). In addition, nonstimulus-induced correlations, as quantified by Equation 2, are indistinguishable from zero during beat and chirp (data not shown, two-tailed sign test, $p > 0.4$). The observed

synchronization evoked by the beat is thus entirely stimulus driven.

The mean firing rate during the entire chirp differs from the mean firing rate during the beat (unpaired t test on each stimulus, median $p < 0.01$ for both $70 < \Delta f < 250$ Hz at 20% contrast and for $80 < \Delta f < 200$ Hz at 10% contrast). The absolute, as well as the relative, difference between the mean firing rate during the beat and during the chirp is small (median of differences < 20 Hz for beat frequencies above 100 Hz, median of relative difference about 0.1 and less, Figure 4C). Furthermore, in 79% of the stimuli recorded from single units, the mean firing rate during the chirp was smaller than the one during the beat, whereas in the remaining 21% it is the other way around (10% and 20% contrast, $50 \leq \Delta f \leq 200$ Hz, $n = 740$). In contrast, correlation was reduced by the chirps in 98% of the stimuli. As a consequence, changes in mean firing rate are only weakly correlated with changes in spike correlation ($r = 0.14$, $p < 0.001$).

As a final check for our hypothesis that high-frequency beats synchronize P-units while transient large chirps desynchronize them, we recorded the summed activity of the whole population of electroreceptor afferent fibers using hook electrodes at the posterior branch of the anterior lateral line nerve (see Experimental Procedures). Examples of such recordings are shown in Figure 5. The beat evokes an oscillating population response, presumably arising from the summation of spikes synchronously locked to the beat. A large chirp causes an abrupt breakdown of this synchronous response back to baseline level that corresponds to the desynchronized spiking activity observed in the single- and dual-unit recordings. The population response closely resembles the firing rates obtained from the single-unit recordings using 1 ms kernels.

We use the temporal standard deviation of the population response in order to quantify the amplitude of its oscillation. At high beat frequencies this measure indicates the degree of synchrony among spikes from the entire population of trunk P-unit afferents. At low beat

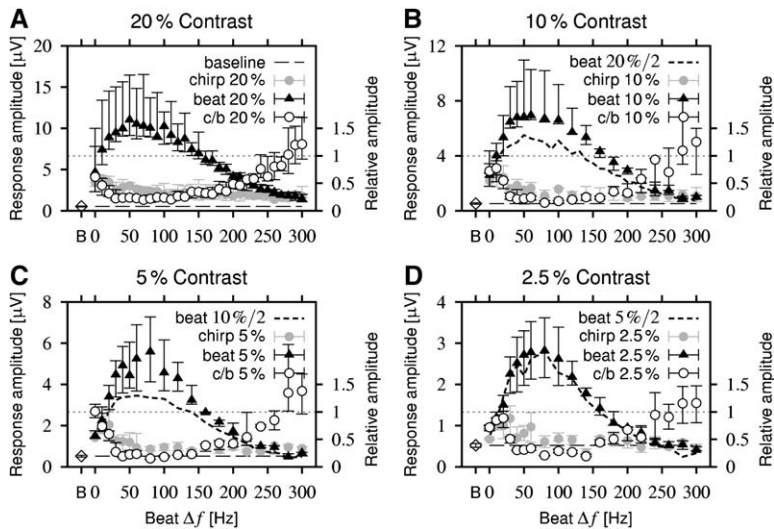


Figure 6. Summary of Recordings from the Trunk Electroreceptor Nerve for Large-Chirp Stimuli

Plotted are median values of the standard deviation of the population response as a measure of its amplitude computed during the beat (black triangles) and chirp (gray circles) with the error bars marking the 1. and 3. quartile. The data points were measured at 5, 10, 20, 30, ... 300 Hz beat frequency at four different contrasts as indicated. The open circles are the relative responses of the chirp divided by beat; the fine dashed lines mark a ratio of one. The dashed line in (B), (C), and (D) is the median of responses to the beat of the previous contrast divided by two. The diamond and the horizontal dashed line denote the standard deviation of the population response during baseline activity.

frequencies this measure reflects the common modulation of the P-unit firing rate, since this also generates some correlation between electroreceptors if analyzed on a slow timescale. Figure 6 summarizes this measure of population activity as a function of beat frequency for four different contrasts.

These experiments confirm our findings from the single and dual P-unit recordings with the amplitude of the population response rising rapidly to a peak at about 50 Hz beat frequency and declining gradually to baseline values at about 250 Hz; interestingly, 250 Hz is near the maximum expected sex difference in EOD frequencies. The strong oscillations evoked by beats are reduced by large chirps for beat frequencies up to 240 Hz at 20% contrast (one-tailed Wilcoxon test, $p < 0.001$, $n = 20$), 220 Hz at 10% contrast ($p < 0.05$, $n = 6$), and 200 Hz at 5% contrast ($p < 0.05$, $n = 6$) (no test possible at 2.5% contrast, since $n = 4$ is too small). Decreasing the contrast reduces the population response during beats less than expected from the equivalent linear reduction by a factor of two (dashed lines), and even at contrasts as low as 2.5%, the large chirps clearly cause an interruption of the beat response. The number of P-units on the head is approximately equal to that on the trunk (Carr et al., 1982); the entire population of P-units can therefore be even more sensitive than demonstrated here. Thus, a sensitive assay of about half the P-unit population (for receptors on the fish's trunk) demonstrates that even weak high-frequency beats can synchronize P-units and that this synchronization is transiently lost during the large chirps.

The mean level of the population response is significantly smaller during the chirps than during the beats at 20% contrast and beat frequencies between 60 and 180 Hz only (two-tailed Wilcoxon test, $p < 0.05$, $n = 20$). At lower contrasts there is no significant difference of the mean population response. Note, however, that this measure is very vulnerable to low-frequency noise.

Synchronization by Small Chirps

At beat frequencies that arise during same sex encounters, (<50 Hz) both males (mainly) and females emit small

chirps—probably as an aggression signal (Zupanc, 2002). Small chirps transiently raise the EOD frequency by 30–150 Hz for about 20 ms and only slightly reduce the EOD amplitude by about 2% (Zupanc and Maler, 1993; Engler et al., 2000; Bastian et al., 2001). The resulting EOD amplitude modulation is a fast signal interrupting the slower beat (see Figure 7A for two examples and Benda et al., 2005 for details).

A low-frequency beat modulates the firing of P-units (Figure 7B). As previously reported (using instantaneous firing frequency as a measure; Benda et al., 2005), small chirps at the trough of the beat produce a fast upstroke in the EOD AM and evoke a transient increase in firing rate that overshoots the maximum response during the beat (Figures 7B and 7C, left column, computed using convolution with a 1 ms Gaussian as above). In contrast, the mean firing rate during the beat hardly differs from that during the chirp. The increased firing rate within a short time window suggests that the P-unit correlation might also be altered during a small chirp (see below).

A small chirp that occurs during the peak of the beat generates a downstroke in the EOD AM, and the electroreceptors respond with a strong decrease in firing rate that undershoots the minimum response during the beat and often results in a short period of silence (right column in Figures 7B and 7C). This decrease in firing rate certainly results in an increased synchrony among the spikes, this time caused by a synchronous absence of spikes. Note also that the firing rate computed with 1 ms wide kernels (black line) deviates from the 5 ms firing rate (gray line) during the chirps only (arrows in Figure 7C).

The population response behaves in exactly the same way (Figure 7D). During the beat it follows the EOD amplitude modulation, but during the small chirps the population response is transiently increased or decreased relative to the response to the beat.

A summary of all the recorded responses to small chirps confirms this observation (Figure 8). The transiently increased and/or decreased firing rate in response to a small chirp can be quantified by the standard deviation of the time course of the firing rate as a measure of its modulation depth (Figure 8A). For beat

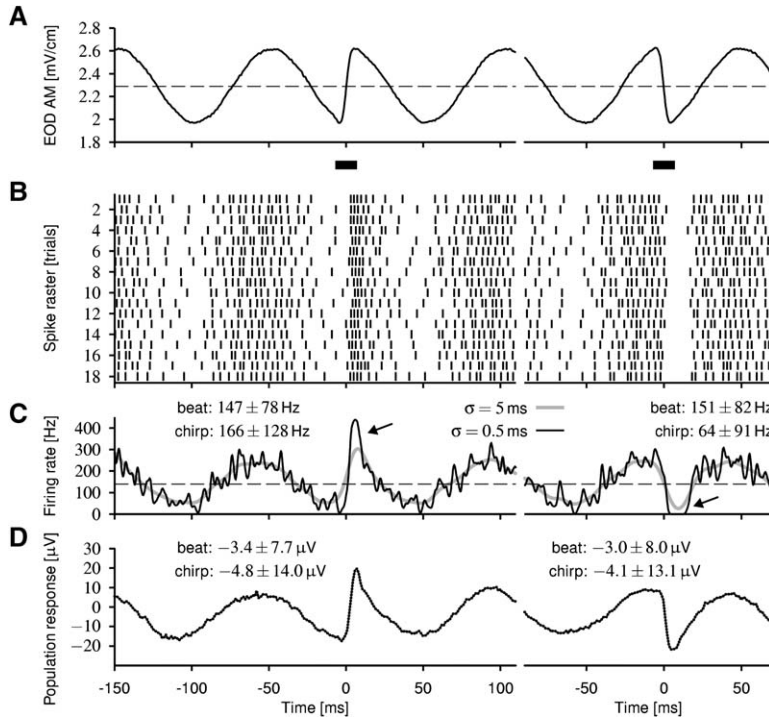


Figure 7. Small Chirps Transiently Enhance Single-Unit as well as Population Response
(A) The stimulus is a beat with frequency $\Delta f = 10$ Hz and 20% contrast with two small chirps at $t = 0$ (thick horizontal bars) occurring in the trough of the beat (left column) and at the peak of the beat (right column). The dashed line marks the baseline EOD amplitude.

(B) Spike raster obtained from a single-unit recording.

(C) Firing rate computed from the spike trains in (B) using Gaussian kernels with standard deviations of 1 ms (black line) and 5 ms (gray line). The transiently increased or decreased firing rate during the chirps can be interpreted as an increase in synchrony of spiking and nonspiking activity, respectively (arrows). The dashed line is the baseline firing rate.

(D) The population response to similar stimuli recorded from the trunk electroreceptor nerve of another fish.

frequencies below about 30 Hz, the modulation depth of the response during the chirp is up to two times larger than the one during the beat (one-tailed Wilcoxon test, $p \ll 0.001$, $\bar{n} = 409$) as we reported in Benda et al. (2005). A very similar, but much stronger, effect can be seen in the correlation between the spike trains

(Figure 8B). At very low beat frequencies (5 Hz), the P-unit correlation during the chirp is about 3-fold higher than that during the beat. The P-unit correlation induced by a small chirp is significantly larger than that induced by the beat for beat frequencies up to 30 Hz inclusively (one-tailed Wilcoxon test, $p \ll 0.001$, $\bar{n} = 375$).

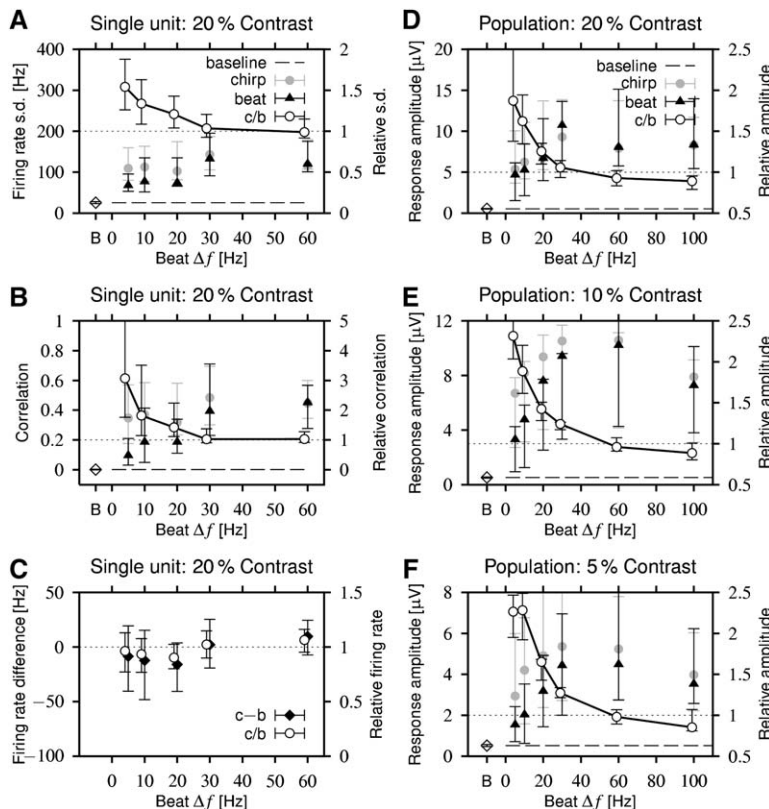


Figure 8. Summary of Responses to Small Chirps

The open circles are the median of the relative responses of the chirp divided by the beat. The diamond and the dashed line denote the corresponding values measured during baseline activity. Plotted are medians with the error bars marking the 1. and 3. quartile. (A) The temporal standard deviation of the firing rate computed from single-unit recordings using Gaussian kernels with 1 ms standard deviation shows that the modulation depth of the firing rate during the chirp (gray circles) is larger than that during the beat (black triangles) at beat frequencies below about 30 Hz. (B) The correlation of the same spike trains as in (A) shows a stronger difference. (C) The difference of the mean firing rate between chirps and beats (black diamonds) and the corresponding ratio (open circles). (D-F) The population response at 5%, 10%, and 20% contrast as indicated resembles both the standard deviation of the firing rate (A) and the correlation (B) from the single-unit recordings.

Although the mean firing rate during the beat and small chirps differs significantly (two-tailed Wilcoxon test, $p < 0.05$, $\bar{n} = 319$), the average difference is small (less than 20 Hz, Figure 8C), and much smaller than the corresponding standard deviation (ranging from 32 Hz at $\Delta f = 60$ Hz to 67 Hz at $\Delta f = 5$ Hz). In other words, there is still an almost equal chance of a small chirp to increase (41% at $\Delta f = 5$ and 10 Hz, $n = 1111$) or decrease (59%) the mean firing rate, whereas correlation is increased in 90% of the stimuli. Changes in mean firing rate and changes in spike correlation are therefore uncorrelated ($r = 0.008$, $p = 0.93$).

The recordings of the population response show the very same pattern. The lower the beat frequency, the stronger the response amplitude during small chirps relative to the response amplitude during the beat (Figures 8D–8F). This enlarged amplitude of the population response to the small chirps suggests a transiently increased or decreased firing rate that results in a short period of increased synchrony of the spiking activity—either by a common high firing rate or by the common absence of spikes. At 5%, 10%, and 20% contrast, the response amplitude is significantly larger during the small chirp than during the beat for beat frequencies up to 30 Hz inclusively (one-tailed Wilcoxon test, $p < 0.05$; 20% contrast: $n = 70$; 10%: $n = 11$; 5%: $n = 8$). The mean population response does not significantly differ between small chirps and beats (two-tailed Wilcoxon test, $p < 0.001$, $n = 57$), except at 20% contrast and a beat frequency of 100 Hz.

Overall, these results demonstrate that, in addition to the modest increase or decrease in firing rate caused by small chirps on a background of low frequency beats, there is an additional even stronger and highly consistent effect: these transient signals also increase spike correlations among P-units.

Discussion

Synchronous spiking within populations of neurons is suggested to play a key role in forming cell assemblies (Laurent, 1996; Harris, 2005), binding (Singer and Gray, 1995), top-down processing (Engel et al., 2001), and perhaps sensory coding (Ishikane et al., 2005; Friedrich et al., 2004). Our data on the representation of weakly electric fish communication signals in a population of electroreceptor neurons demonstrates that both transient desynchronization as well as synchronization can code for important signals within the same population of neurons. A female of the weakly electric fish *A. leptorhynchus* that is close to a male receives a high-frequency beat (between about 50 to 250 Hz). The electroreceptor neurons lock to this oscillation in exactly this range of beat frequencies and became strongly synchronized. However, a large chirp emitted by the male in response to such high-frequency beats transiently desynchronizes the electroreceptor population. On the contrary, during same-sex encounters, the beat frequency is lower (less than 50 Hz) and the P-units are much less synchronized. In this context, a small chirp transiently enhances synchrony of the P-unit population. Small changes in the mean firing rate that are also induced by the chirps do not, however, reliably indicate the presence of either small or large chirps.

Rapid spike-frequency adaptation reduces the gain for slow (<30 Hz) beats. Small chirps introduce a high-frequency stimulus (about 100 Hz) that is faster than the adaptation dynamics and thus evoke a transiently enhanced firing-rate response (Benda et al., 2005), consequently increasing spike correlation. For the same reason, fast beats (between 50 and 200 Hz) synchronize the P-unit population, since they are faster than all adaptation processes (Xu et al., 1996) and thus get transmitted with high gain (Benda and Herz, 2003; Chacron et al., 2005a). A large chirp causes the effective beat to become irregular and of reduced amplitude, causing the electroreceptor response to desynchronize. The frequency modulation of the chirping fish's EOD is unlikely to contribute to the desynchronization since we observed it at low contrasts (Figure 6D) where temporal aspects of the EOD of the receiving fish are no longer influenced by the other EOD. Future modeling studies will investigate how P-unit dynamics control the degree of synchrony.

Electrical stimulation of P-unit afferents evokes a mixture of EPSPs and inhibitory postsynaptic potentials (IPSPs) in pyramidal cells that are the main targets of P-units (Maler et al., 1981). Berman and Maler (1998) showed that the postsynaptic potentials (PSPs) sum up to either a depolarization in most basilar pyramidal cells (E-cells) or a hyperpolarization in nonbasilar pyramidal cells (I-cells) in response to a 200 Hz tetanic stimulation, corresponding to P-units locking to a 200 Hz beat. The resulting PSP originating from 50 to 1500 P-units (L.M., unpublished data) could therefore be approximated by simply adding up P-unit-evoked PSP waveforms. The first, AMPA receptor-mediated component of the EPSP in E-cells is just about 1 ms wide, and the first, GABA-A receptor-mediated component of the IPSP in I-cells can peak as early as 2 ms after a stimulus pulse (Berman and Maler, 1998). Therefore, the summed potentials of these fast components of the PSPs should be similar to both the firing rate obtained by convolving the spike trains with 1 ms standard deviation Gaussian kernels (e.g., Figure 3C) and the population response (Figure 5C), where the individual spikes averaged over one EOD cycle constitute the kernels. The effect of slower PSPs (NMDA receptor-mediated; Berman and Maler, 1998; L.M., unpublished data) could then be approximated by the firing rate computed using wider kernels and adding (EPSPs) or subtracting (IPSPs) this firing rate from the 1 ms firing rate. This very simplified picture of the synaptic input to the pyramidal cells suggests that it is very likely that synchrony of the P-units on a 1 ms timescale is accessible by the pyramidal cells through fast PSPs, and that the slower IPSPs reduce the response to slower signals like the ones evoked by slow beat frequencies. This view is also in agreement with the high-pass filter properties of pyramidal cells reported by Chacron et al. (2003) for communication-like stimulation.

We have shown, based on dual-unit recordings, that synchronization of P-units is solely induced by common stimulation with amplitude modulations of the EOD, and not by interactions between the neurons. Quantifying such stimulus-driven spike synchronization by a correlation coefficient like Equation 1 involves two timescales: a short one, measuring coincident spikes, and a longer

one, for computing the mean firing rate as a reference value for chance-level coincidences. The short timescale is set by the width of the kernels (1 ms) we convolved the spike trains with. As discussed in the previous paragraph, these kernels match the fast components of PSPs in the P-unit's target cells. On the contrary, the long timescale is implicitly given by the time window used for computing the correlation coefficient. This timescale has no natural counterpart in the pyramidal cells' PSPs. Some of these PSPs are of similar or even shorter duration as the chirps, and thus shorter than the time window we used for computing the correlation coefficient. The correlation of P-units we reported for slow beat frequencies might therefore overestimate the correlation relevant for driving pyramidal cells. A comparison of the firing rate computed using the 1 ms kernels with a firing rate based on wider kernels (5 ms) resembling some of the slower PSPs (Figures 2, 3, and 7, gray lines) might be closer to reality than the correlation coefficient. In this picture, the slower PSPs would naturally define a timescale that separates slow stimuli that are translated as a population rate code from fast stimuli, like fast beats and small chirps, that give rise to synchrony. Note that the correlation coefficient equation (Equation 2) quantifying noise correlations (internally generated correlations not induced by the stimulus) requires only a single short timescale for both detecting coincident spikes and computing a reference firing rate across trials.

In the context of communication signals, pyramidal cells express high-pass filter properties, with a cutoff frequency at about 20 Hz (Chacron et al., 2003, 2005b). They are known to be feature detectors that are most informative about fast upstrokes (E-cells) or downstrokes (I-cells) in EOD AMs (Krahe et al., 2002). Both properties are perfectly suited to detect small chirps in the P-unit population response. On the other hand, the firing rate of pyramidal cells is typically less than 60 Hz and coherence rapidly decreases for stimulus frequencies above about 60 Hz (Chacron et al., 2005b), whereas vector strength can be close to one for 100 Hz beats (Chacron et al., 2003). These response properties to high-frequency stimuli suggest that synchrony of P-units and their desynchronization by large chirps might not be decoded by single pyramidal cells. Instead, the information might be distributed over the population of pyramidal cells (Krahe et al., 2002), and well-characterized feedback loops (Berman and Maler, 1999) might also play an important role in shaping the response (Doiron et al., 2003). The change in the "beat" network state induced by desynchronization might enable downstream circuitry to discriminate large chirps from baseline activity. Behavioral studies (Zupanc et al., 2005; J. Lewis, personal communication) and physiological responses of central electrosensory neurons to artificial chirp-like stimuli (delivered without a beat and thus not naturally occurring in a communication context; Metzner and Heiligenberg, 1991; Heiligenberg et al., 1991) suggest that decoding circuitry for chirps is present. Although synchrony is hypothesized to play a major role in cortical information processing (Singer and Gray, 1995), the specific neuronal mechanisms employed for a readout of synchrony or desynchronization are still under investigation (e.g., Azouz and Gray, 2003). Future analysis of the recoding of synchrony and asynchrony in the simple

but well-characterized and accessible circuitry of the electrosensory system will give valuable insight into the function of the cortex as well.

Visual stimulation temporarily desynchronizes the EEG (event-related desynchronization, Vijn et al., 1991) or multiunit activity (van der Togt et al., 2006). Often this desynchronization is immediately followed by re-synchronization (Woertz et al., 2004). Rodriguez et al. (1999) suggested that EEG desynchronization "reflects a process of active uncoupling of the underlying neuronal ensembles that is necessary to proceed from one cognitive state to another." Although the scope of our data is not directly comparable to human EEG studies (see also Munk et al., 1996), our results nevertheless demonstrate that desynchronization can be more than a switch from one synchronous state to another; transient desynchronization can be used by a neural system as a code for a short but important signal (i.e., the large chirp emitted by a male to a female in this study, and the null-direction of direction-selective retinal ganglion cells investigated by Ackert et al., 2006). Furthermore, in a different social context the same population of neurons was synchronized by another, even shorter, type of communication signal (the small chirp used during encounters of the same sex). More generally, our study emphasizes that the *change* from synchrony to asynchrony or vice versa might be a relevant signal for the next level of neural processing, in contrast with synchrony alone.

Experimental Procedures

Electrophysiology

Single and dual P-unit recordings, as well as whole nerve recordings, were made from the posterior branch of the anterior lateral line nerve ganglion; this contains only electroreceptor afferent fibers innervating electroreceptors on the fish's trunk (Maler et al., 1974). For surgical exposure of the trunk nerve, fish were anesthetized (MS-222, Sigma-Aldrich, St. Louis, MO). After surgery fish were immobilized (Flaxedil, Sigma) and transferred into a tank (28°C) where they were respirationally supported by a constant flow of oxygenated water through the mouth. Action potentials from single P-unit afferents were routinely recorded in vivo with sharp glass micropipettes (100 M Ω) that were advanced into the nerve with piezoelectric microdrives (Inchworm IW-711, Burleigh, Fishers, NY; and MM3A, Kleindiek nanotechnik, Germany). The potential between the micropipette and the reference electrode, which was placed on the nerve close to the electrode, was amplified (Axoprobe 1A; Axon Instruments, Union City, CA), band-pass filtered (0.45–7 kHz; PC1; TDT, Alachua, FL), and notch filtered at 60 Hz and the fish's EOD frequency (Ultra-Q Pro; Behringer, Willich, Germany). Population activity was recorded using a pair of hooks made out of silver wire, high-pass filtered at 2 Hz, and differentially amplified (2015F; Intronix, Bolton, ON). The response of the population to 100 Hz beat stimuli vanished after cutting the nerve, demonstrating that the recorded activity indeed originated from the electroreceptor afferents and not from the applied stimulus. All experimental protocols were approved by the University of Ottawa Animal Care Committee.

The EOD unperturbed by the stimulus was recorded between head and tail of the fish using two vertical carbon rods (11 cm long, 8 mm diameter). The transdermal voltage constituting the stimulus picked up by the P-units was estimated by two silver wires coated with nail polish, 1 cm apart, placed perpendicular to the side of the fish. Both EOD voltages were amplified and low-pass filtered at 5 kHz (2015F; Intronix, Bolton, ON). Stimuli were attenuated (PA4; TDT, Alachua, FL), isolated (Model 2002; A-M Systems, Carlsborg, WA), and delivered by two stimulation electrodes (30 cm long, 8 mm diameter carbon rods) placed 10 cm on either side of the fish, parallel to its longitudinal axis. Amplitude modulations were

generated by multiplying the AM signal with the fish's EOD (MT3; TDT, Alachua, FL).

The extracellular potential, the EOD, the transdermal potential, and the attenuated stimulus were digitized at 20 kHz with a 12 bit Multi-IO-board (PCI-MIO-16E-4; National Instruments, Austin, TX) on an Intel Pentium IV 1.8 GHz Linux PC. Spike and EOD detection, stimulus generation and attenuation, and preanalysis of the data were performed online during the experiment within our OEL (Online Electrophysiology Laboratory) software.

Data from 16 adult *A. leptorhynchus* (10–23 cm, ten males) were used for single-unit recordings of large chirps. Dual-unit recordings were obtained from four fish (11–17 cm, three males) and population recordings were obtained from a different set of four fish (11–15 cm, two males). The single-unit recordings of small chirps are the same as described in Benda et al. (2005) (nine fish, 12–16 cm).

Protocols and Data Analysis

Amplitude modulation stimuli were composed of a beat of a given frequency with a chirp in the middle of the stimulus. The duration of the initial segment with the beat was 100 ms or at least one beat period, and the final segment lasted 30 ms or at least one beat period. The middle segment containing the chirp had a duration of one beat period plus 77 ms. The large chirp—also known as the type-I chirp (Engler et al., 2000; Bastian et al., 2001) or HiC (Triefenbach and Zakon, 2003)—was modeled as a Gaussian increase of EOD frequency with an maximum increase of 600 Hz (the chirp size) and a width at 10% height of either 19.2 or 24 ms. In addition, the EOD amplitude was decreased by the same Gaussian by 75% (50% for the population recordings). The width of small chirps (type-II chirp or LoC) at 10% height was 14 ms, and their size was 30, 60, 100, 122, or 153 Hz (see Benda et al., 2005 for details).

Mean firing rate, standard deviation of the firing rate, and spike correlation of single-unit activity in response to chirps were computed within a small time window ranging from –5 to 15 ms for large chirps and from –3 to 13 ms for small chirps relative to the center of the chirp at $t = 0$. The offset of 5 ms accounted for delays of the response. For analyzing the response to the beat, a time window starting at –80 ms or earlier relative to the center of the chirp and ending at –24 ms was used. The length of the window was adjusted to an integer multiple of the beat period. Baseline activity was quantified by cutting about 8 s of recorded activity into “trials” of 400 ms duration.

Mean firing rate is the number of spikes within the time window of interest divided by the width of the window and the number of trials. The time course of the firing rate was computed by convolving the spike trains with Gaussian kernels with a standard deviation of either 1 or 5 ms and averaging over trials. The 1 ms kernel corresponds to the fast component of PSPs evoked by P-units in their target cells, whereas the 5 ms kernel represents a lower bound of the width of slower components of the PSPs (Berman and Maler, 1998). From the resulting time series the mean and the standard deviation was calculated.

Spike correlation was quantified as the correlation coefficient

$$r_{ij} = \frac{\langle (s_i - \langle s_i \rangle_t)(s_j - \langle s_j \rangle_t) \rangle_t}{\sqrt{\langle (s_i - \langle s_i \rangle_t)^2 \rangle_t} \sqrt{\langle (s_j - \langle s_j \rangle_t)^2 \rangle_t}} \quad (1)$$

of pairs of spike trains convolved with Gaussian kernels of 1 ms standard deviation, $s_i(t)$ and $s_j(t)$, averaged over all possible pairs ij . All averages $\langle \cdot \rangle_t$ in Equation 1 are taken over time t . Equation 1 is closely related to the reliability measure suggested by Schreiber et al. (2003). Correlation of spike trains obtained from dual-unit recordings were computed by averaging over the convolved spike trains from simultaneously recorded pairs of spike trains. Averaging over all nonsimultaneously recorded spike trains resulted in the “shuffled” correlation.

A different and commonly used definition of the correlation coefficient for dual recordings measures correlations that cannot be attributed to the stimulus (“noise correlations”):

$$q = \left\langle \frac{\langle (s_i - \langle s_i \rangle_t)(r_i - \langle r_i \rangle_t) \rangle_t}{\sqrt{\langle (s_i - \langle s_i \rangle_t)^2 \rangle_t} \sqrt{\langle (r_i - \langle r_i \rangle_t)^2 \rangle_t}} \right\rangle_t \quad (2)$$

Therein, $s_i(t)$ and $r_i(t)$ are the spike trains of the two neurons from trial i , respectively, and the average $\langle \cdot \rangle_t$ is taken over the trials i . Thus,

$\langle s_i \rangle$ and $\langle r_i \rangle$ are the firing rates of the two neurons. Equation 2 is obtained by averaging the normalized joint peristimulus time histogram $J(t_1, t_2)$ (Aertsen et al., 1989; Brody, 1999) over time with $t = t_1 = t_2$.

From the raw recordings of the nerve potential, we removed the contamination by the EOD using a sliding average over one EOD cycle as described in Figure 5. The “population response” was then obtained by averaging this signal over trials. The amplitude of the population response was computed as its standard deviation, since the standard deviation is a more robust measure compared with the difference between peaks and troughs. The time window for analyzing the population response to large chirps ranged from –6 to 8 ms relative to the chirp. Large chirps induce a reduction of the response amplitude, and therefore, a time window smaller than the width of a chirp better separates the properties of the response to the chirp from the response to the beat. Since the population response is a continuous signal, it was possible to use a smaller window for this than for the spike data.

Acknowledgments

We are very grateful to Hartmut Schütze for suggesting the hook electrode recordings of the population activity. This work was supported by a CIHR grant to L.M. and A.L.

Received: May 5, 2006

Revised: July 24, 2006

Accepted: August 3, 2006

Published: October 18, 2006

References

- Ackert, J.M., Wu, S.H., Lee, J.C., Abrams, J., Hu, E.H., Perlman, I., and Bloomfield, S.A. (2006). Light-induced changes in spike synchronization between coupled ON direction selective ganglion cells in the mammalian retina. *J. Neurosci.* 26, 4206–4215.
- Aertsen, A., Diesmann, M., and Gewaltig, M.O. (1996). Propagation of synchronous spiking activity in feedforward neural networks. *J. Physiol. (Paris)* 90, 243–247.
- Aertsen, A.M.H.J., Gerstein, G.L., Habib, M.K., and Palm, G. (1989). Dynamics of neuronal firing correlation: Modulation of “effective connectivity”. *J. Neurophysiol.* 61, 900–917.
- Azouz, R., and Gray, C.M. (2003). Adaptive coincidence detection and dynamic gain control in visual cortical neurons in vivo. *Neuron* 37, 513–523.
- Bar-Yosef, O., Rotman, Y., and Nelken, I. (2002). Responses of neurons in cat primary auditory cortex to bird chirps: Effects of temporal and spectral context. *J. Neurosci.* 22, 8619–8632.
- Bastian, J. (1981). Electrolocation I. How electroreceptors of *Apteronotus albifrons* code for moving objects and other electrical stimuli. *J. Comp. Physiol. [A]* 144, 465–479.
- Bastian, J., Schniederjan, S., and Nguyenkim, J. (2001). Arginine vasotocin modulates a sexually dimorphic communication behavior in the weakly electric fish *Apteronotus leptorhynchus*. *J. Exp. Biol.* 204, 1909–1923.
- Benda, J., and Herz, A.V.M. (2003). A universal model for spike-frequency adaptation. *Neural Comput.* 15, 2523–2564.
- Benda, J., Longtin, A., and Maler, L. (2005). Spike-frequency adaptation separates transient communication signals from background oscillations. *J. Neurosci.* 25, 2312–2321.
- Berman, N.J., and Maler, L. (1998). Inhibition evoked from primary afferents in the electrosensory lateral line lobe of the weakly electric fish (*Apteronotus leptorhynchus*). *J. Neurophysiol.* 80, 3173–3196.
- Berman, N.J., and Maler, L. (1999). Neural architecture of the electrosensory lateral line lobe: adaptations for coincidence detection, a sensory searchlight and frequency-dependent adaptive filtering. *J. Exp. Biol.* 202, 1243–1253.
- Bernander, O., Koch, C., and Usher, M. (1994). The effect of synchronized inputs at the single neuron level. *Neural Comput.* 6, 622–641.
- Brody, C.D. (1999). Correlations without synchrony. *Neural Comput.* 11, 1537–1551.

- Carr, C.E., Maler, L., and Sas, E. (1982). Peripheral organization and central projections of the electrosensory nerves in gymnotiform fish. *J. Comp. Neurol.* *211*, 139–153.
- Chacron, M.J., Longtin, A., and Maler, L. (2001). Negative interspike interval correlations increase the neuronal capacity for encoding time-dependent stimuli. *J. Neurosci.* *21*, 5328–5343.
- Chacron, M.J., Doiron, B., Maler, L., Longtin, A., and Bastian, J. (2003). Non-classical receptive field mediates switch in a sensory neuron's frequency tuning. *Nature* *423*, 77–81.
- Chacron, M.J., Maler, L., and Bastian, J. (2005a). Electroreceptor neuron dynamics shape information transmission. *Nat. Neurosci.* *8*, 673–678.
- Chacron, M.J., Maler, L., and Bastian, J. (2005b). Feedback and feedforward control of frequency tuning to naturalistic stimuli. *J. Neurosci.* *25*, 5521–5532.
- Dan, Y., Alonso, J.-M., Usrey, W.M., and Reid, R.C. (1998). Coding of visual information by precisely correlated spikes in the lateral geniculate nucleus. *Nat. Neurosci.* *1*, 501–507.
- Doiron, B., Chacron, M.J., Maler, L., Longtin, A., and Bastian, J. (2003). Inhibitory feedback required for network oscillatory responses to communication but not prey stimuli. *Nature* *421*, 539–543.
- Engel, A.K., König, P., Kreiter, A.K., Schillen, T.B., and Singer, W. (1992). Temporal coding in the visual cortex: new vistas on integration in the nervous system. *Trends Neurosci.* *15*, 218–226.
- Engel, A.K., Fries, P., and Singer, W. (2001). Dynamic predictions: oscillations and synchrony in top-down processing. *Nat. Rev. Neurosci.* *2*, 704–716.
- Engler, G., Fogarty, C.M., Banks, J.R., and Zupanc, G.K.H. (2000). Spontaneous modulations of the electric organ discharge in the weakly electric fish, *Apteronotus leptorhynchus*: a biophysical and behavioral analysis. *J. Comp. Physiol. [A]* *186*, 645–660.
- Ermentrout, B. (1996). Type I membranes, phase resetting curves, and synchrony. *Neural Comput.* *8*, 979–1001.
- Friedrich, R.W., Habermann, C.J., and Laurent, G. (2004). Multiplexing using synchrony in the zebrafish olfactory bulb. *Nat. Neurosci.* *7*, 862–871.
- Galán, R.F., Fourcaud-Trocmé, N., Ermentrout, G.B., and Urban, N.N. (2006). Correlation-induced synchronization of oscillations in olfactory bulb neurons. *J. Neurosci.* *26*, 3646–3655.
- Galarreta, M., and Hestrin, S. (2001). Spike transmission and synchrony detection in networks of GABAergic interneurons. *Science* *292*, 2295–2299.
- Greschner, M., Bongard, M., Rujan, P., and Ammermüller, J. (2002). Retinal ganglion cell synchronization by fixational eye movements improves feature estimation. *Nat. Neurosci.* *5*, 341–347.
- Hagedorn, M., and Heiligenberg, W. (1985). Court and spark: electric signals in the courtship and mating of gymnotoid fish. *Anim. Behav.* *33*, 254–265.
- Hagiwara, S., Szabo, T., and Enger, P.S. (1965). Electroreceptor mechanisms in a high-frequency weakly electric fish, *Sternarchus albifrons*. *J. Neurophysiol.* *28*, 784–799.
- Harris, K.D. (2005). Neural signatures of cell assembly organization. *Nat. Rev. Neurosci.* *6*, 399–407.
- Heiligenberg, W., and Partridge, B.L. (1981). How electroreceptors encode JAR-eliciting stimulus regimes: Reading trajectories in a phase-amplitude plane. *J. Comp. Physiol. [A]* *142*, 295–308.
- Heiligenberg, W., Keller, C.H., Metzner, W., and Kawasaki, M. (1991). Structure and function of neurons in the complex of the nucleus electrosensorius of the gymnotiform fish *Eigenmania*: Detection and processing of electric signals in social communication. *J. Comp. Physiol. [A]* *169*, 151–164.
- Hirabayashi, T., and Miyashita, Y. (2005). Dynamically modulated spike correlation in monkey inferior temporal cortex depending on the feature configuration within a whole object. *J. Neurosci.* *25*, 10299–10307.
- Hopkins, C.D. (1976). Stimulus filtering and electroreception: Tuberosum electroreceptors in three species of gymnotoid fish. *J. Comp. Physiol. [A]* *111*, 171–207.
- Ishikane, H., Gangi, M., Honda, S., and Tachibana, M. (2005). Synchronized retinal oscillations encode essential information for escape behavior in frogs. *Nat. Neurosci.* *8*, 1087–1095.
- Krahe, R., Kreiman, G., Gabbiani, F., Koch, C., and Metzner, W. (2002). Stimulus encoding and feature extraction by multiple sensory neurons. *J. Neurosci.* *22*, 2374–2382.
- Kramer, B. (1999). Waveform discrimination, phase sensitivity and jamming avoidance in a wave-type electric fish. *J. Exp. Biol.* *202*, 1387–1398.
- Lamme, V.A.F., and Spekreijse, H. (1998). Neuronal synchrony does not represent texture segregation. *Nature* *396*, 362–366.
- Laurent, G. (1996). Dynamical representation of odors by oscillating and evolving neural assemblies. *Trends Neurosci.* *19*, 489–496.
- Lindner, B., Doiron, B., and Longtin, A. (2005). Theory of oscillatory firing induced by spatially correlated noise and delayed inhibitory feedback. *Phys. Rev. E. Stat. Nonlin. Soft Matter Phys.* *72*, 061919. Published online December 29, 2005. 10.1103/PhysRevE.72.061919.
- Maler, L., Finger, T., and Karten, H.J. (1974). Differential projections of ordinary lateral line receptors and electroreceptors in the gymnotid fish, *Apteronotus (Sternarchus) albifrons*. *J. Comp. Neurol.* *158*, 363–382.
- Maler, L., Sas, E.K.B., and Rogers, J. (1981). The cytology of the posterior lateral line lobe of high-frequency weakly electric fish (Gymnotidae): Dendritic differentiation and synaptic specificity in a simple cortex. *J. Comp. Neurol.* *195*, 87–139.
- Metzner, W., and Heiligenberg, W. (1991). The coding of signals in the electric communication of the gymnotiform fish *Eigenmannia*: From electroreceptors to neurons in the torus semicircularis of the midbrain. *J. Comp. Physiol. [A]* *169*, 135–150.
- Meyer, J.H., Leong, M., and Keller, C.H. (1987). Hormone-induced and maturational changes in electric organ discharges and electroreceptor tuning in the weakly electric fish *Apteronotus*. *J. Comp. Physiol. [A]* *160*, 385–394.
- Munk, M.H.J., Roelfsema, P.R., König, P., Engel, A.K., and Singer, W. (1996). Role of reticular activation in the modulation of intracortical synchronization. *Science* *272*, 271–274.
- Nelson, M.E., and MacIver, M.A. (1999). Prey capture in the weakly electric fish *Apteronotus albifrons*: sensory acquisition strategies and electrosensory consequences. *J. Exp. Biol.* *202*, 1195–1203.
- Nelson, M.E., Xu, Z., and Payne, J.R. (1997). Characterization and modeling of P-type electrosensory afferent responses to amplitude modulations in a wave-type electric fish. *J. Comp. Physiol. [A]* *181*, 532–544.
- Oestreich, J., Dembrow, N.C., George, A.A., and Zakon, H.H. (2006). A “sample-and-hold” pulse-counting integrator as a mechanism for graded memory underlying sensorimotor adaptation. *Neuron* *49*, 577–588.
- Perez-Orive, J., Bazhenov, M., and Laurent, G. (2004). Intrinsic and circuit properties favor coincidence detection for decoding oscillatory input. *J. Neurosci.* *24*, 6037–6047.
- Ratnam, R., and Nelson, M.E. (2000). Nonrenewal statistics of electrosensory afferent spike trains: implications for the detection of weak sensory signals. *J. Neurosci.* *20*, 6672–6683.
- Robertson, L.C. (2003). Binding, spatial attention and perceptual awareness. *Nat. Rev. Neurosci.* *4*, 93–102.
- Rodriguez, E., George, N., Lachaux, J.-P., Martinerie, J., Renault, B., and Varela, F.J. (1999). Perception's shadow: long distance synchronization of human brain activity. *Nature* *397*, 430–433.
- Scheich, H., Bullock, T.H., Robert, H., and Hamstra, J. (1973). Coding properties of two classes of afferent nerve fibers: high frequency electroreceptors in the electric fish, *Eigenmannia*. *J. Neurophysiol.* *36*, 39–60.
- Schreiber, S., Fellous, J.M., Whitmer, D., Tiesinga, P., and Sejnowski, T.J. (2003). A new correlation-based measure of spike timing reliability. *Neurocomputing* *52–54*, 925–931.
- Singer, W. (1999). Neuronal synchrony: a versatile code for the definition of relations? *Neuron* *24*, 49–65.
- Singer, W., and Gray, C.M. (1995). Visual feature integration and the temporal correlation hypothesis. *Annu. Rev. Neurosci.* *18*, 555–586.

- Tamás, G., Buhl, E.H., Lörincz, A., and Somogyi, P. (2000). Proximally targeted GABAergic synapses and gap junctions synchronize cortical interneurons. *Nat. Neurosci.* 3, 366–371.
- Thiele, A., and Stoner, G. (2003). Neuronal synchrony does not correlate with motion coherence in cortical area MT. *Nature* 421, 366–370.
- Triefenbach, F., and Zakon, H. (2003). Effects of sex, sensitivity and status on cue recognition in the weakly electric fish *Apteronotus leptorhynchus*. *Anim. Behav.* 65, 19–28.
- van der Togt, C., Kalitzin, S., Spekreijse, H., Lamme, V.A., and Super, H. (2006). Synchrony dynamics in monkey V1 predict success in visual detection. *Cereb. Cortex* 16, 136–148.
- Vijn, P.C.M., van Dijk, B.W., and Spekreijse, H. (1991). Visual stimulation reduces EEG activity in man. *Brain Res.* 550, 49–53.
- Volgushev, M., Chistiakova, M., and Singer, W. (1998). Modification of discharge patterns of neocortical neurons by induced oscillations of the membrane potential. *Neuroscience* 83, 15–25.
- Woertz, M., Pfurtscheller, G., and Klimesch, W. (2004). Alpha power dependent light stimulation: dynamics of event-related (de)synchronization in human electroencephalogram. *Brain Res. Cogn. Brain Res.* 20, 256–260.
- Xu, Z., Payne, J.R., and Nelson, M.E. (1996). Logarithmic time course of sensory adaptation in electrosensory afferent nerve fibers in a weakly electric fish. *J. Neurophysiol.* 76, 2020–2032.
- Zakon, H., Oestreich, J., Tallarovic, S., and Triefenbach, F. (2002). EOD modulations of brown ghost electric fish: JARs, chirps, rises, and dips. *J. Physiol. (Paris)* 96, 451–458.
- Zupanc, G.K.H. (2002). From oscillators to modulators: behavioral and neural control of modulations of the electric organ discharge in the gymnotiform fish, *Apteronotus leptorhynchus*. *J. Physiol. (Paris)* 96, 459–472.
- Zupanc, G.K.H., and Maler, L. (1993). Evoked chirping in the weakly electric fish *Apteronotus leptorhynchus*: a quantitative biophysical analysis. *Can. J. Zool.* 71, 2301–2310.
- Zupanc, G.K.H., Sirbulescu, R.F., Nichols, A., and Ilies, I. (2005). Electric interactions through chirping behavior in the weakly electric fish, *Apteronotus leptorhynchus*. *J. Comp. Physiol. [A]* 192, 159–173.